ELSEVIER

Polymer 44 (2003) 3031–3036

polymer

www.elsevier.com/locate/polymer

Real-time monitoring of segmental dynamics during crystallization of poly(L(−)-lactide) by simultaneous DRS/SALS technique

Benjamin D. Fitz*, Saša Andjelić

Department of Polymer and Suture Technologies, Ethicon, a Johnson and Johnson Company, P.O. Box 151, Route 22, West Somerville, NJ 08876-0151, USA

Received 8 November 2002; received in revised form 5 February 2003; accepted 7 February 2003

Abstract

A novel experimental set up consisting of dielectric spectroscopy and small angle light scattering (or potentially any other optical technique used in combination) is introduced. The sample is enclosed in a Dielectric-Optical-Shear (DOS) cell capable of precisely controlling temperature and thickness. This method allows for *simultaneous* in situ, real-time monitoring of the changes in the molecular dynamics and corresponding development of supramolecular structure of a given polymer system during various time-sensitive processes. The DOS cell is utilized to investigate relaxation phenomena related to the glass transition, T_g, of poly(L(−)-lactide) during isothermal crystallization under quiescent, partially constrained conditions. A decrease in T_g was observed in situ via a shift in dipolar relaxation to higher frequency (confirmed calorimetrically, ex situ). The shift was most rapid in the spherulitic impingement stage of crystallization, at approximately 30% overall crystallinity.

Keywords: Dielectric spectroscopy; Small-angle light scattering; Poly(L-lactide)

1. Introduction

Dielectric Spectroscopy (DS) has been used for several decades to study macromolecular segmental relaxation (dipolar relaxation) and translational motions of migrating charges (ionic conductivity) in an applied electrical field for variety of polymer systems-nominally stable materials, and in materials whose properties are time-sensitive [1–4]. Although DS has a long history, recently a resurgence of interest has occurred due to progress in instrumentation and sensor developments [5–9]. As a consequence of these achievements in DS technology, the term broadband DS has been used lately by the research community to indicate the application of the technique over many (in some cases 16) decades of frequency [10–12]. In spite of this impressive range, the molecular-level interpretation of the dielectric response in polymer systems, particularly those involving time-sensitive structural changes, remains a challenging task. Frequently the DS signal is obscured by multiple relaxation phenomena and experimental artifacts. To overcome such problems, independent measurements of the event by an appropriate supporting technique is necessary. Thus it is desirable to use DS simultaneously with other complementary techniques. In the literature, such types of measurements have been scarce [13–17].

In the present study a novel experimental system consisting of *simultaneous* DS and Small Angle Light Scattering (SALS) is introduced to study physical phenomena in poly(L(−)-lactide), PLLA. The SALS method has been used to study the development of supramolecular structures, including characterizing nucleation and spherulite growth in semi-crystalline polymers [18] and nucleation and grain growth in amorphous block copolymers [19]. In addition, optical transmission measurements can be used to obtain crystallization kinetics [20].

In our previous communication [21], we described a reduction in the glass transition temperature of PLLA that had been crystallized under partially constrained conditions, where the polymer was prevented from shrinking during crystallization. We found that the T_g-depression increased with increasing degree of crystallization, %X, or crystallization temperature, T_c. On the other hand, unconstrained PLLA samples exhibited the conventional trend of increasing T_g with %X or T_c. Although the difference in T_g between samples prepared by the two methods was large, as much as

* Corresponding author. Tel.: +1-908-218-2828; fax: +1-908-218-2840.
E-mail address: bfitz@ethus.jnj.com (B.D. Fitz).

0032-3861/03/$ - see front matter © 2003 Elsevier Science Ltd. All rights reserved.
doi:10.1016/S0032-3861(03)00161-7

30 °C, the melting point, heat of fusion and overall degree of crystallinity were not influenced. No degradation was found during crystallization of PLLA under these conditions—NMR showed no increase in monomer content, and GPC showed no reduction in molecular weight. This phenomenon was explained by an increase in the net free volume in the amorphous phase, as the increasing crystal volume fraction has a higher density than the amorphous fraction, which is not able to contract to maintain its nominal density.

As a continuation of the previous work, we attempt to monitor T_g changes in real time during crystallization utilizing our recently built DS/SALS instrument. This study is intended to provide a deeper insight into the relationship between the T_g-depression and crystallinity. A second goal is to learn if there is a particular stage of crystal development where this effect has its onset.

2. Experimental section

2.1. Materials

Poly(L-(−) lactide) homopolymer (hereafter, referred to as PLLA) was prepared at Ethicon by a tin catalyzed ring-opening bulk polymerization. The polymer, after grinding and heating in vaccuo to remove unreacted monomer, had an inherent viscosity of 1.75 dl/g in hexaflouroisopropanol at 25 °C at a concentration of 0.1 g/dl. The PLLA weight average molecular weight, M_w, was 117,000 g/mol, with a number average molecular weight, M_n, of 50,000 g/mol (by GPC). Prior to use the samples were stored under vacuum; during testing, exposure to ambient atmosphere was limited. Selected samples were examined for molecular weight and inherent viscosity reduction following the experimental procedure, and no significant reductions were found (<2%). NMR analysis at the end of crystallization cycles revealed that no monomer generation occurred during this process.

2.2. Dielectric-optical-shear (DOS) cell

For simultaneous DS and SALS measurements, a custom-modified parallel-plate shear apparatus (Linkam CSS 450, Linkam Scientific Instruments Ltd, Tadworth, Surrey, UK) was used to host a sample while precisely controlling the sample temperature and thickness. In order to use the Linkam cell to perform dielectric measurements, a significant modification of the original set up was required. We replaced the usual quartz windows with metalized, but transparent, indium-tin-oxide-coated quartz windows. A guard electrode was prepared by selectively etching portions of the ITO-coating from the windows. Insulating polytetrafluroethylene sheets were used to insure electrical isolation of the sample cell from the rest of the shear cell. Finally, thin electrode leads were carefully guided outside the DOS enclosure and attached to the DS instrument. The additional function of this cell is to apply a variety of shear modes—step, steady or oscillatory, at a wide range of shear rates and overall strains. The aperture in the parallel windows for viewing or passing the SALS laser was located 7.5 mm from the center of the windows, and had a diameter of 2.8 mm.

2.3. Small angle light scattering

For SALS measurements a 20 mW HeNe laser (Uniphase, Manteca, CA) with $\lambda = 0.633$ μm was used as the light source. The light was directed through an uncoated right-angle glass prism, followed by the compensator (quartz half-wave retardation plate) and the first polarizer. The laser beam then reached the sample, which was enclosed in a custom-modified optical Linkam CSS 450 Cambridge Shearing System supplied with a precise temperature control unit. The light emerging from the sample passed through a broadband beam sampler (splitter), where approximately 5% of the light was redirected and focused into a silicon photodiode. This photo-detector was used to measure the changes in transmitted laser intensity as a function of time. By recording the voltage displayed by an amplifier connected to the detector output, the transmission, I/I_0, was measured. A relative extent of crystallinity may be derived from relative changes in transmission as crystallization proceeds: $1 - (I(t) - I_\infty)/(I_0 - I_\infty)$, where I_0 and I_∞ are the initial and final transmission values. The major portion of the light beam, unaffected by the sampler, advanced to the analyzer. From there, the Hv (incident light polarized vertically and scattered light polarized horizontally) scattering pattern was projected onto a high quality paper screen using a 50 mm dielectric mirror.

Coordinates in the projection plane were determined by two angles, θ and μ. The scattering vector was calibrated using the four concentric circles method as described elsewhere [22]. The scattering profiles were recorded by a NEC TI324A CCD industrial high-resolution monochrome camera, equipped with a Nikon 28 mm lens and positioned on the optical rails. The images were captured and analyzed using Image Pro Plus® (version 4.0) software. The entire setup was mounted on a research grade optical table supported by vibrational isolators.

2.4. Dielectric relaxation spectroscopy (DRS)

In this study, Dielectric relaxation spectroscopy (hereafter, referred to as DRS), the part of DS that concerns dipole relaxation, was utilized. Electrical leads from the DOS cell were attached to a Hewlett-Packard HP4284A precision LCR meter, having a frequency range from 20 Hz to 1 MHz. The samples were in the form of circular films (diameter, 3 cm) pressed between the electrodes. The electrode gap (thus sample thickness) between the metalized windows was 400 μ. Frequency sweeps from 100 Hz to 1 MHz, with ten points per decade, requires about one minute to perform; this measurement time is much shorter

than the time-scale of crystallization in the polymers under investigation.

2.5. Differential scanning calorimetry (DSC)

Calorimetric results were obtained on TA Instruments Model 2910 MDSC, with a dry nitrogen purge. The heating rate was 10 °C/min.

2.6. Wide angle X-ray diffraction (WAXD)

The overall percent crystallinity in the polymer was determined by Wide angle X-ray diffraction (WAXD). X-ray measurements were carried out on a Siemens Hi-Star™ diffractometer using Cu Kα radiation at the wavelength of 1.542 Å. The X-ray beam was incident normal to the polymer film surface. The deconvolution of the X-ray images and the calculation of crystallinity were conducted using the DIFFRAC PLUS™ software developed by Siemens. The parameters of the amorphous peak were obtained from quenched, completely amorphous PLLA, then later used on the semi-crystalline PLLA patterns. Gaussian functions were used for fitting the crystal reflections.

2.7. Experimental procedure

Prior to use, the samples were stored under nitrogen. All samples were melted at 210 °C for 10 min to erase any thermal or mechanical history. After 5 min at 210 °C, when the sample was entirely molten, the upper lid of the DOS cell was lowered to achieve our desired sample-thickness of about 400 μm (verified after each experiment). Following the melting step, the samples were quenched to the desired crystallization temperature, and then allowed to quiescently crystallize. The sample enclosed in the DOS cell was restricted from volumetric contraction (shrinking) during crystallization (constrained conditions) because of the polymers affinity to the walls of the vessel containing it. In other words, since the polymer wets the walls of the DOS cell, during crystallization, as the more dense crystalline phase develops, the polymer must do one of three things to accommodate the overall density change: (1) delaminate from the walls of the cell (thus, becoming free to shrink), (2) form voids, or (3) increase the free volume in the amorphous phase. After each crystallization run the samples were found to be adhering to the walls of the DOS cell, and on closer inspection, no voids were visible. Following each experiment, selected samples were examined for molecular weight and inherent viscosity reduction and no significant reductions were found ($<2\%$).

3. Results and discussion

In this section we present results obtained from *simultaneous* DRS/SALS measurements during isothermal crystallization of PLLA. In the first part of the discussion we focus on the changes in dipole relaxation spectra during crystallization conducted at different isothermal conditions. In the second part of the discussion, we analyze the range of scattering patterns obtained by SALS, describing the formation of spherulitic structures. Finally, crystallization kinetics obtained by dielectric and scattering methods are reviewed.

3.1. Molecular dynamics during isothermal crystallization of PLLA by DRS

First we should establish the rational for our experimental conditions. They are bounded by the available DRS frequency range, and by the temperature range of crystallization of PLLA. We begin by noting that the dipolar loss peak in the frequency domain is related to the glass transition of a given polymer system. At test temperatures near, or slightly above calorimetric T_g, the segmental relaxation is slow, hence the dipole relaxation peak occurs at low frequency. However, with an increase in temperature, the location of the dipolar relaxation moves to higher frequency. For semicrystalline polymers, there is an optimal experimentally-accessible temperature range where the loss peak is located in the frequency window of the instrument, and where crystallization kinetics are sufficiently slow to allow frequency sweeps to be completed (i.e. for frequency range 100 Hz to 1 MHz a frequency sweep takes between 45 and 60 s) without significant structural changes occurring during a measurement. Having established the experimental conditions of interest, in Fig. 1(A)–(C) we present dipole loss data of PLLA in the frequency domain as a function of crystallization time at three isothermal crystallization temperatures: 75, 85 and 90 °C, respectively. As mentioned above, these samples were initially melted, followed by rapid cooling to the desired temperature where crystallization is carried out. Due to the fact that PLLA can be easily supercooled upon applying moderate cooling steps, the first spectra shown in Fig. 1(A)–(C) (noted '0' time) belong to a fully amorphous polymer. The onset of crystallization is marked by the first drop in the intensity of the dipole relaxation peak. The decrease in the peak intensity is related to the portion of polymer chains that become dialectically inactive, due to their incorporation in the crystal lattice or incorporation into a 'rigid amorphous phase' [24]. With progress in crystallization, for all isothermal conditions (Fig. 1(A)–(C)), the intensity of the dipole peak gradually decreases, but the most probable relaxation time, τ or location of the peak is initially unchanged. Interestingly, in a later stage of crystallization, a significant shift of τ towards higher frequency is observed. This unusual behavior of a crystallizing polymer has not, to our knowledge, been previously reported in the literature. Moreover, the opposite trend is well-known in polymer crystallization. Historically, the explanation for the crystallization-slowed relaxation process is that the crystals act as

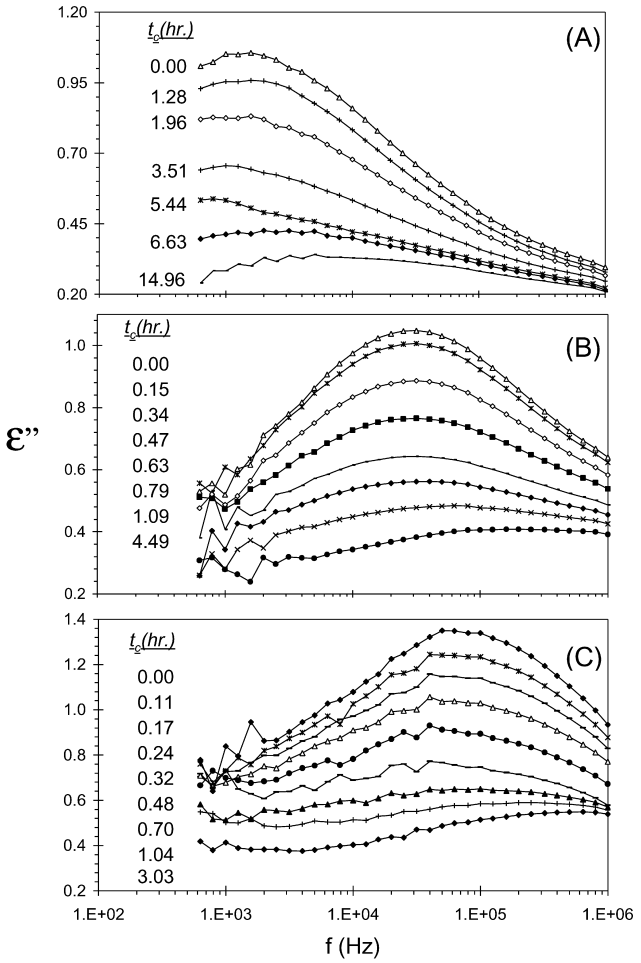

Fig. 1. Dipolar relaxation in crystallizing PLLA during isothermal crystallization at: (A) 75, (B) 85, and (C) 90 °C.

constraints on the amorphous relaxation process [23,25]. In the present study, the shift of the dipole peak to higher frequency is a direct, in situ observation of a decrease in the polymer's glass transition temperature. Such a T_g-depression in a confined system was found previously [21], but in that work the T_g-depression was characterized ex situ.

In Fig. 2, the frequency at the maximum loss peak is plotted versus crystallization time for PLLA crystallized isothermally at 90 °C (see Fig. 1(C)). Also in this figure are relative crystallization kinetics by DRS. The method of determining crystallization kinetics by monitoring the decrease in relaxed (low frequency) permittivity, ε_0',

$$\text{crystallinity}(t) = \frac{\varepsilon_0'(0) - \varepsilon_0'(t)}{\varepsilon_0'(0) - \varepsilon_0'(\infty)} \quad (1)$$

where $\varepsilon_0'(t)$ denotes the approximate value of relaxed permittivity at time t (taken as ε' (1000 Hz)), while $\varepsilon_0'(0)$ and $\varepsilon_0'(\infty)$ are its initial and final values, respectively, and has been reported earlier [26–28]. For example, the crystallization of the biodegradable polyester, poly(*p*-dioxanone), has been characterized by DRS and compared

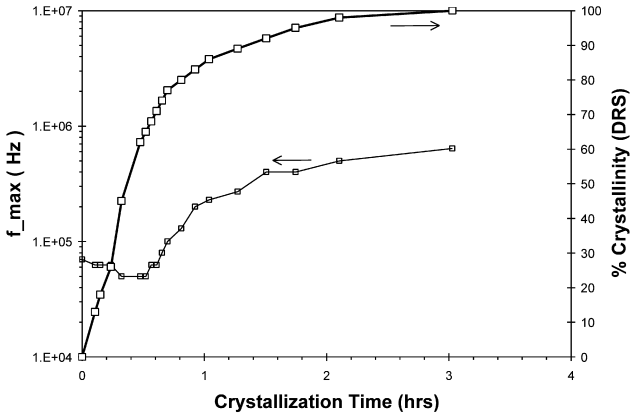

Fig. 2. Frequency of maximum dielectric loss and relative crystallinity (by DRS) vs. isothermal crystallization time at 90 °C.

with crystallization kinetics determined by other real-time monitoring techniques [29]. Fig. 2 shows that up to ~60% of relative crystallinity, the dipole peak position is unchanged, however, at later crystallization times, a gradual shift of the peak to higher frequencies is clearly evident.

The dielectric loss peak is also shown to broaden in Fig. 1. Estimates of this broadening were made by fitting the loss peaks to the well-known KWW functional form [1]. For the 85 °C crystallization of PLLA (Fig. 1(B)), the initial peak had a KWW β parameter of 0.37, and the final peak had a β of 0.19. Broadening of the segmental relaxation is common for crystallizing polymers [1–4].

In order to further explore the effect of crystallinity on the glass transition behavior of PLLA, we determined the glass transition temperature (DSC) and the corresponding degree of crystallinity (WAXD) for a series of samples that had been partially crystallized in the DOS cell at 90 °C then were quenched to arrest crystallization, and characterized off-line. The relationship between T_g and degree of crystallinity obtained on this series of quenched samples is shown in Fig. 3. This figure shows the decrease in T_g with crystallinity. As crystallinity increases in the constrained samples, the excess free volume in the polymer increases with crystallization, resulting in further T_g-depression. At degrees of crystallinity between 25 and 35% (WAXD), optical microscopy shows this crystallization regime to be where spherulitic impingement occurs. This crystallization range is coincident with the onset of the dipolar relaxation shift to higher frequencies. The transition in dielectric loss peak frequency (thus, T_g) vs. crystallization time in this crystallinity range appears to be related to these supramolecular structural developments.

3.2. Monitoring of supramolecular development by SALS

Simultaneously with DRS measurements, we collected SALS patterns of PLLA that capture formation and growth of spherulitic structures in this system. SALS images taken at different times during the isothermal crystallization of

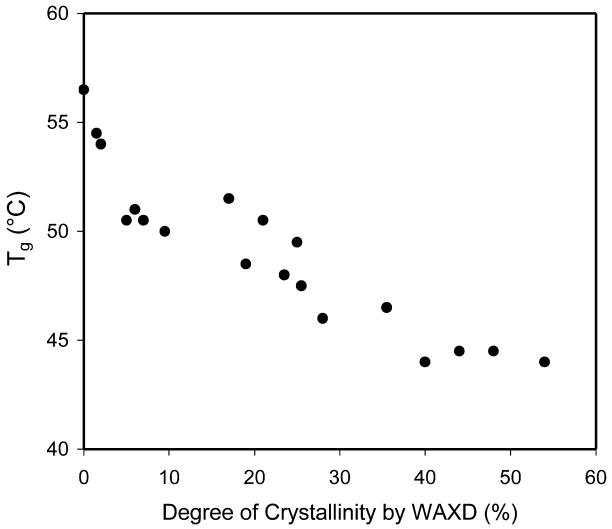

Fig. 3. Glass transition temperature (calorimetric) vs. %crystallinity (WAXD) for PLLA isothermal crystallization at 90 °C under constrained conditions.

PLLA at 90 °C are presented in Fig. 4(A)–(C). At early times in the crystallization process, a four-lobed pattern of low intensity was noticed, indicating the initial development of spherulitic structure. These patterns, interestingly, precede the first detection of crystallinity by DRS, suggesting that SALS is a more sensitive technique to follow the onset of crystallization. With an increase in crystallinity, the scattering patterns become notably smaller and more intense, reflecting the growth of existing spherulites and an increasing number of new ones.

In order to compute structural parameters from the SALS patterns, we integrated the scattering pattern along the 45° azimuthal line. The resulting curves for a given time-series are presented in Fig. 5. The average size of spherulites is

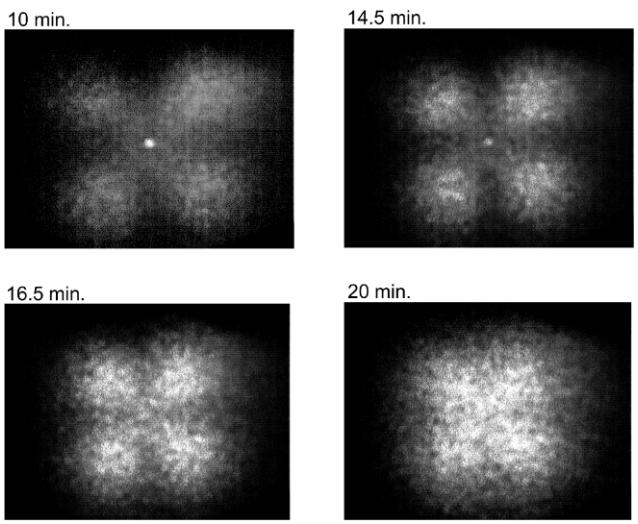

Fig. 4. SALS images taken during isothermal crystallization of PLLA at 90 °C at selected crystallization times.

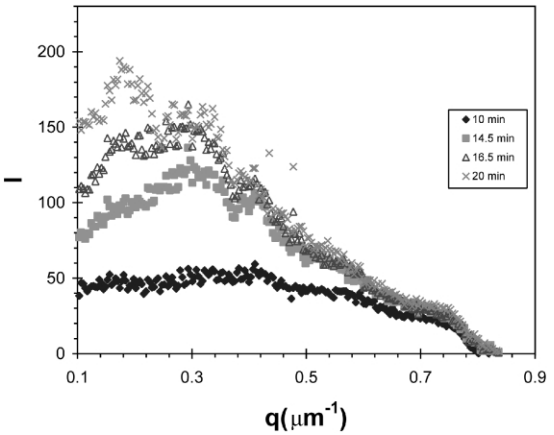

Fig. 5. Depolarized light scattering profiles of SALS images in Fig. 4, along 45°.

obtained from Ref. [18]

$$R = \frac{4.1\lambda}{4\pi}\left[\sin\left(\frac{\vartheta_{max}}{2}\right)\right]^{-1} = \frac{4.1}{q_{max}} \quad (2)$$

where λ is the wavelength of the light, θ_{max} is the scattering angle at which the intensity is maximum, or alternately, q_{max} is the location in scattering vector, q, where the intensity is maximum. From the integrated SALS patterns in Fig. 5, the spherulitic development in PLLA ranges from an average spherulite diameter of 20.5 μ at 10 min, to 42.5 μ at 20 min.

3.3. Crystallization kinetics by DRS and SALS transmission measurements

In Fig. 6 the normalized extent of crystallization determined using Eq. (1) is plotted for the 90 °C isothermal runs. For comparison, we include in the same graph kinetic data obtained simultaneously using the decay in light transmission through the DOS cell. The results from the two techniques diverge noticeably. The light transmission data show faster kinetics than those observed by DRS. These

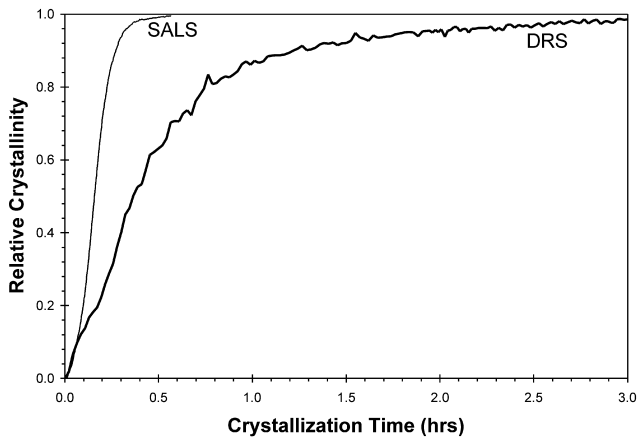

Fig. 6. Relative crystallinity via normalized reduction in dielectric constant (DRS) and normalized reduction in light transmission (SALS) as a function of crystallization time for PLLA crystallized 90 °C.

results reveal that the more sensitive technique for measuring overall crystallization kinetics in PLLA is DRS, while the more sensitive measure of the onset of crystallization, as mentioned above, is SALS. For PLLA crystallized at 90 °C, the spherulites impinge at ~30% crystallinity (via WAXS; ~60% via DRS). At this impingement stage the light transmission has decayed to its minimum, while there remains a significant amount of amorphous material to be crystallized—the latter crystallization process continues to be detected by DRS. Depending on the sequence of events during structure formation in the crystallization of a polymer, these diverse techniques may yield an agreement in kinetics: an example of an agreement between DRS and transmission measurements of crystallinity was found in our previous study of the crystallization kinetics of poly(*p*-dioxanone) by SALS, DRS, SAXS, WAXD, and DSC [20].

4. Conclusions

A novel experimental technique based on simultaneous dielectric and SALS measurements capable of monitoring time-sensitive processes is introduced. This technique was used to investigate a previous finding of a reduction in the glass transition temperature of PLLA, crystallized under constrained conditions. We have observed the glass transition change during isothermal crystallization in situ, and in real time, via monitoring shifts in the dielectric loss peak. The segmental dipolar relaxation was found to shift to higher frequencies in the crystallization range where spherulitic impingement occurs, at approximately 30% overall crystallinity.

References

[1] McCrum NG, Read BE, Williams G. Anelastic and dielectric effects in polymer solids. New York: Wiley; 1967.
[2] Hedvig P. Dielectric spectroscopy of polymers. New York: Wiley; 1977.
[3] Senturia SD, Sheppard NF. Adv Polym Sci 1986;80:1.
[4] (a) Williams G. In: Runt JP, Fitzgerald JJ, editors. Dielectric spectroscopy of polymeric materials. Washington, DC: American Chemical Society; 1997. p. 3–65. Chapter 1. (b) Schönhals A. In: Runt JP, Fitzgerald JJ, editors. Dielectric spectroscopy of polymeric materials. Washington, DC: American Chemical Society; 1997. p. 81–107. Chapter 3.
[5] Kranbuehl DE, Delos SE, Jue PK. Polymer 1986;27:11.
[6] Casalini R, Fioretto D, Livi A, Lucchesi M, Rolla PA. Phys Rev B 1997;56:3016.
[7] Andjelić S, Mijović J, Bellucci F. J Polym Sci Polym Phys Ed 1998; 36:641.
[8] Andjelić S, Mijović J. Macromolecules 1998;31:8463.
[9] Fitz B, Mijović J. J Phys Chem B 2000;104(51):12215.
[10] Kremer F, Boese D, Fetters L. J Non-cryst Solids 1991;131–133:728.
[11] Brand R, Lunkenheimer P, Loidl A. Phys Rev B: Condens Matter 1997;56(10):R5713.
[12] Fitz B, Mijović J. Macromolecules 2000;33(3):887.
[13] Fournier J, Williams G, Duch C, Aldridge GA. Macromolecules 1996; 29:7097.
[14] Andjelić S, Fitz B, Mijović J. Macromolecules 1997;30:5239.
[15] Tombari E, Salvetti G, Johari GP. J Chem Phys 2000;113(16):6957.
[16] Sics I, Ezquerra TA, Nogales A, Balta-Calleja FJ, Kalnins M, Tupureina V. Biomacromolecules 2001;2(2):581.
[17] Mijović J, Sy J. Macromolecules 2002;35:6370.
[18] Stein RS, Rhodes MB. J Appl Phys 1960;31:1873.
[19] Newstein MC, Garetz BA, Balsara NP, Chang MY, Dai HJ. Macromolecules 1998;31:64.
[20] Abuzaina F, Fitz BD, Andjelić S, Jamiolkowski DD. Polymer 2002; 43:4699.
[21] Fitz BD, Jamiolkowski DD, Andjelić S. Macromolecules 2002;35: 5869.
[22] Dai HJ. PhD Dissertation, Polytechnic University, New York; June 1998
[23] Ezquerra TA, Balta-Calleja FJ, Zachmann HG. Polymer 1994;35: 2600.
[24] Iannace S, Nicolais L. J Polym Sci Polym Phys Ed 1997;35:911.
[25] Nogales A, Ezquerra TA, Garcia JM, Balta-Calleja FJ. J Polym Sci Polym Phys Ed 1999;37:37.
[26] Williams G. Adv Polym Sci 1979;33:59.
[27] Boyd RH. J Polym Sci Polym Phys Ed 1983;21:505.
[28] Andjelić S, Fitz BD. J Polym Sci: Part B Polym Phys 2000;38:2436.
[29] Andjelić S, Jamiolkowski D, McDivitt J, Fischer J, Zhou J, Wang Z, Hsiao B. J Polym Sci: Part B Polym Phys 2001;39:153.